and octonary signals have been used to conclude that pulse shaped signals perform significantly better than CPFSK signals both in absence and in presence of a symbol timing error. It has also been shown that the improvement is more significant for LD and DC receivers, and at higher values of $M$.

**Table 3** MAXIMUM ALLOWABLE NORMALISED TIMING ERROR

| | | Pulse shaped | | CPFSK | |
|---|---|---|---|---|---|
| $M$ | Receiver | $BT$ | $\Delta_{max}$ | $BT$ | $\Delta_{max}$ |
| 4 | LD and DC | 2 | 0·277 | 2 | 0·145 |
| 4 | CDDD | 2 | 0·401 | 2 | 0·332 |
| 8 | LD and DC | 3 | 0·199 | 3·5 | 0·038 |
| 8 | CDDD | 3 | 0·276 | 3 | 0·137 |

Pulse shaped signals perform better than CPFSK signals because they have smooth phase variations during symbol transitions compared with those piecewise variations of the latter. Smooth phase variations of pulse shaped signals introduce less ISI due to bandlimiting and also introduce a lower phase error in the presence of a timing error than CPFSK signals. The improvement with LD and DC receivers is more significant because their decisions depend on ISI at both the beginning and the end of any interval, whereas those of the CDDD receiver depend on only one ISI component. Even though the advantages of pulse shaping have been demonstrated here by using a raised cosine pulse, similar full-response baseband pulses, such as the one-half cycle sinusoid (1-HCS) pulse [3], would also provide similar improvements.

*31st March 1992*

J. P. Fonseka (*School of Engineering and Computer Science, The University of Texas at Dallas, Richardson, TX 75083-0688, USA*)

**References**


1 EKANAYAKE, N., and FONSEKA, J. P.: 'Error rate performance of narrow-band multilevel CPFSK signals', *IEE Proc. F*, 1987, **134**, (2), pp. 151–158
2 PAWULA, R. F.: 'On the theory of error rates for narrow-band digital FM', *IEEE Trans.*, 1981, **COM-29**, pp. 1634–1642
3 ANDERSON, J. B., AULIN, T., and SUNDBERG, C. E.: 'Digital phase modulation' (Plenum Press, New York, 1986)
4 FONSEKA, J. P., and EKANAYAKE, N.: 'Comparison of three detection techniques for M-ary CPFSK with modulation index 1/M'. Proc. IEEE Global Telecommun. Conf., Atlanta, Georgia, 1984, pp. 22.6.1–22.6.7


613

## 70Gbit/s FIBRE BASED SOURCE OF FUNDAMENTAL SOLITONS AT 1550nm

S. V. Chernikov, D. J. Richardson, R. I. Laming, E. M. Dianov and D. N. Payne

*Indexing terms: Soliton transmission, Optical communication*

The generation of a 70Gbit/s CW soliton train with a mark-space ratio of 1 : 11 from a fibre system based on the nonlinear propagation of a dual-frequency beat-signal within dispersion decreasing fibre is reported.

Ultrahigh bit rate sources of soliton pulses capable of operating in the gigahertz region are of considerable interest for the next generation of optical fibre telecommunication systems, as well as for optical signal processing. At present mode-locked external-cavity laser diodes [1, 2], gain-switched diodes [3] and, more recently, actively mode-locked erbium-fibre ring lasers [4] have been employed to generate the necessary soliton pulse trains for long-haul transmission experiments at bit rates in the range of 2–10Gbit/s. Recently, an alterative all-optical method of ultrahigh frequency soliton generation has been suggested, based on the nonlinear propagation of a beat signal between two narrow-linewidth lasers in an amplifying fibre or alternatively, a fibre of steadily decreasing dispersion [5, 6]. The technique enables the generation of high-purity soliton pulses at repetition rates ranging from tens to hundreds of Gbit/s (corresponding to the frequency separation of the source lasers). In the first experimental demonstrations of this technique 25ps bunches of solitons at 200GHz [6] and 1 $\mu$s trains of solitons at repetition rates in the range of 80–130GHz [7] were generated in a fibre of steadily decreasing dispersion. We report for the first time the generation of a truly CW train of high purity solitons around 1·551 $\mu$m in a dispersion tailored fibre system.

The experimental configuration is illustrated in Fig. 1. Two, pigtailed single-frequency DFB lasers DFB1 and DFB2 were combined using a 50 : 50 coupler. The combined signal was then passed through a polarisation-sensitive isolator (isolator 1) into an erbium-doped fibre amplifier (EDFA) with counter-propagating pump. Polarisation controllers were included in both inputs to the combining coupler to maximise and equalise the relative intensities of the input signals. The laser wavelength separation could be varied between 0 and 2·5nm by independently varying the temperature of the diodes. The EDFA was pumped using a Ti : sapphire laser operating at 978nm which was coupled into the EDFA via a WDM coupler. The input pump power was accurately stabilised using a servo-circuit and Bragg cell placed in front of the launch optics. The amplified diode-laser beat-signal emerging from the EDFA was passed through a second polarisation insensitive isolator (isolator 2). Up to 300mW of amplified signal was available at the isolator output. A 1km section of dispersion-shifted fibre (DSF) ($|D| < 1·5$ps/nm/km at 1551nm) was spliced to the isolator output, followed by the dispersion-decreasing fibre (DDF) of length 1·6km. The tapered DDF was fabricated using a recently developed technique [8]. The dispersion, measured at 1·55 $\mu$m, decreased from $D = 10$ps/nm/km at the output. The dispersion-length profile was designed to be close to a hyperbolic form. The total system loss was 2dB. In the first experiments, a 90 : 10 coupler was spliced to the DDF output to facilitate real-time monitoring of the pulse train by a background free autocorrelator, optical spectrum analyser and an average power meter.

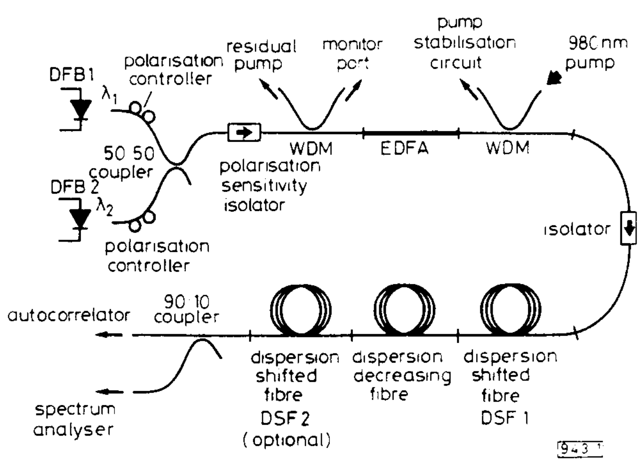


**Fig. 1** *Experimental configuration*

Note: fibre DSF2 was optional and only used during transmission experiments

The implementation we adopted is slightly different to p· · viously published techniques [5, 6] in that we added a sect· of DSF before the DDF. The DSF was used to spectrally enrich the beat signal through four-wave mixing prior to soliton formation and compression in the DDF. This enrichment permitted us to extend the range of application of the particular DDF to lower repetition rates and correspondingly lower input powers than would be possible with the DDF alone. The basic mechanism of soliton train generation however remains the same. A more detailed discussion of the technique is to be found in Reference 9.

The spectrum of a 300mW beat signal from the laser d··de EDFA combination after propagation through the D shown in Fig. 2*a*. Four-wave mixing generates sidebands ~10 dB below the main signal components and was independent of the wavelength separation for separations up to 0·7 nm. Autocorrelation functions measured at the input and

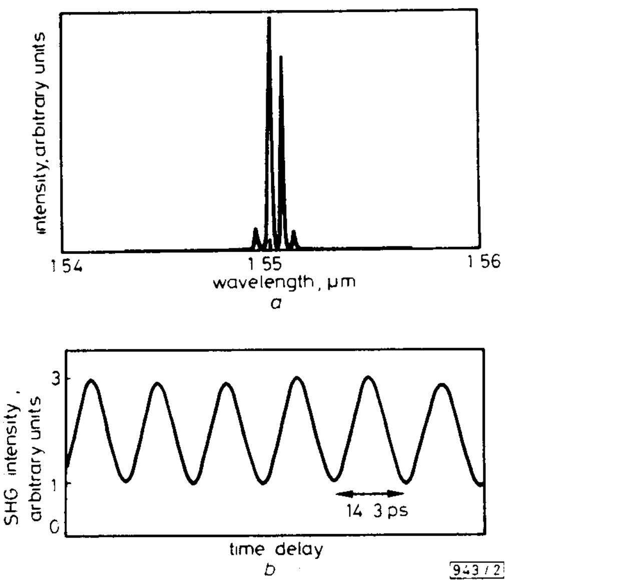


**Fig. 2** *Spectrum and autocorrelation trace of amplified beat signal at end of 1·0 km DSF*

Input signal power was 300 mW
*a* Spectrum
*b* Autocorrelation trace

output of the DSF were fitted well by a sinusoidal beat signal of the form $G(\tau) = 1 + 2\cos^2(\pi R\tau)$, where $R$ is the repetition rate and $\tau$ the time delay, giving a 3 : 1 relation between the maximum to minimum SHG intensity (Fig. 2*b*) for the autocorrelation trace. Following spectral enrichment in the DSF the soliton train was generated in the DDF. Fig. 3*a* and *b* show the spectrum and corresponding autocorrelation function measured at the DDF output for a DFB wavelength separation of 0·57 nm (70 GHz). The autocorrelation trace shows that we have generated a train of well-separated pulses with a period of 14·3 ps. There is no background on the autocorrelation function and the trace is flat between pulses. The individual pulses have a good sech$^2$ form with no pedestal. The half width of the autocorrelation function corresponds to a soliton duration of 1·3 ps. The optical spectrum (Fig. 3*a*)

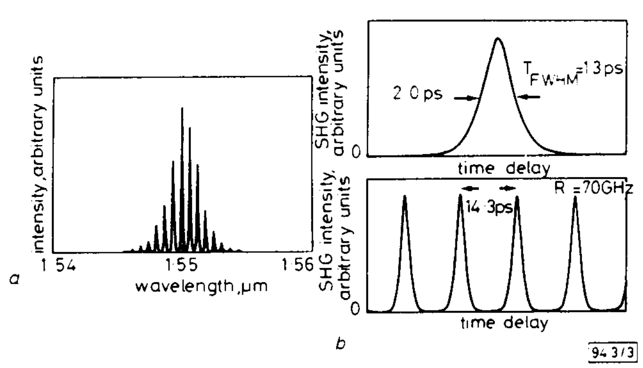


**Fig. 3** *Spectrum and autocorrelation trace of 70 Gbit/s soliton train at output of DDF*

*a* Spectrum
*b* Autocorrelation trace

contains a discrete number of lines separated by ~0·57 nm and corresponds to a 70 GHz periodic signal. The heights of the discrete peaks in the spectrum can be fitted by a continuous envelope which corresponds to the optical spectrum of the individual pulses forming the train. The autocorrelation function and spectrum provide an excellent fit to a train of 70 GHz solitons with durations of 13 ps (corresponding to an MSR of 1 : 11).

Investigation of the system behaviour over the complete range of input beat-signal parameters (frequency separation and average power),* indicates that high-quality soliton trains could be obtained for repetition rates in the range 60–90 Gbit/s with MSRs in the range 1 : 5–1 : 11 from this single configuration.

We also investigated the propagation of pulse trains generated by the system in a further section of dispersion-shifted fibre (DSF2). The fibre, of length 2·2 km and dispersion $D \simeq 1{\cdot}5$ ps/nm/km at 1·55 mm, was spliced directly to the DDF output. Fig. 4*a* and *b* show the autocorrelation trace and spectra of a 65 GHz pulse train at the input and Fig. 4*c* and *d* at the output of DSF2 for a beat-signal power of 190 mW. At this beat-signal frequency and power, soliton formation in the DDF is not fully complete. However, owing to the dispersion mismatch between DDF (at the output) and DSF2, propagation in DSF2 results in further reshaping and compression of the pulses. Note, that the length of DSF2 corresponds to ~2 soliton periods for 2·7 ps pulses and a dispersion of 1·5 ps/nm/km.

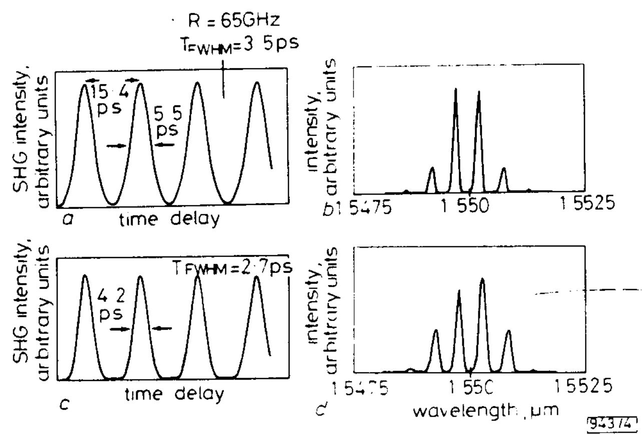


**Fig. 4** *Autocorrelation trace and spectrum of 65 GHz pulse train at output of DDF and after propagation in 2·2 km DSF2*

Input signal power was 190 mW
*a* Autocorrelation for pulse train at DDF output
*b* Spectrum for pulse train at DDF output
*c* Autocorrelation for pulse train after propagation in 2·2 km DSF2
*d* Spectrum for pulse train after propagation in 2·2 km DSF2

In conclusion, we have experimentally generated stable, CW trains of high-purity, fundamental solitons in a dispersion decreasing fibre at 70 Gbit/s, using the technique of soliton-train formation from a dual-frequency beat signal generated by a combination of two DFB diode lasers and an EDFA. We believe that this simple, highly stable and widely tunable all-fibre source has great potential for use in future ultrahigh bit rate telecommunication systems.


*7th May 1992*



S. V. Chernikov and E. M. Dianov (*General Physics Institute, 38 Vavilov Street, 117942, Moscow, Russia*)

D. J. Richardson, R. I. Laming and D. N. Payne (*Optoelectronics Research Centre, Southampton SO9 5NH, United Kingdom*)


## References


1 OLSSON, N. A., ANDREKSON, P. A., SIMPSON, J. R., TANBUN-EK, T., LOGAN, R. A., and WECHT, K. W.: 'Bit-error-rate investigation of two-channel soliton propagation over more than 10000 km', *Electron. Lett.*, 1991, **27**, pp. 695–697

2 MOLLENAUER, L. F., NEUBELT, M. J. HANER, M., LICHMAN, E., EVANGELIDES, S. G., NYMAN, B. M.: 'Demonstration of error-free soliton transmission at 2·5 Gbit/s over more than 14000 km', *Electron. Lett.*, 1991, **27**, pp. 2055–2056

3 NAKAZAWA, M., SUZUKI, K., YAMADA, E., KUBOTA, H., and KIMURA, Y.: '10 GBit/s–1200 km single-pass soliton data transmission using erbium-doped fiber amplifiers'. OFC 92 (San Jose), PD11, 1992, pp. 355–358

4 MOLLENAUER, L. F., LICHTMAN, E., HARVEY, G. T., NEUBELT, M. J., and NYMAN, N. M.: 'Demonstration of error-free soliton transmission


* CHERNIKOV, S. V., MAMYSHEV, P. V., DIANOV, E. M., RICHARDSON, D. J., LAMING, R. I., and PAYNE, D. N.: 'CW soliton train generation in the repetition rate range 60–90 GHz using a dispersion decreasing fibre', submitted to *Soviet Lightwave Communications*

over more than 15000 km at 5 Gbit/s single/channel and over more than 11 000 km at 10 Gbit/s in two channel WDM', *Electron. Lett.*, 1992, **28**, pp. 792–794
5 DIANOV, E. M., MAMYSHEV, P. V., PROKHOROV, A. M., and CHERNIKOV, S. V.: 'Generation of a train of fundamental solitons at a high repetition rate in optical fibre', *Opt. Lett.*, 1989, **14**, pp. 1008–1010
6 MAMYSHEV, P. V., CHERNIKOV, S. V., and DIANOV, E. M.: 'Generation of fundamental soliton trains for high-bit-rate optical fibre communication lines', *IEEE J. Quantum Electron.*, 1991, **27**, pp. 2347–2355
7 CHERNIKOV, S. V., TAYLOR, J. R., MAMYSHEV, P. V., and DIANOV, E. M.: 'Generation of soliton train in optical fibre using two CW single-mode diode lasers', *Electron. Lett.*, 1992, **28**, (10), pp. 931–932
8 BOGATYREV, V. A., *et al.*: 'Single-mode fibre with chromatic dispersion varying over the length', *J. Lightwave Technol.*, 1991, **LT-9**, pp. 561–566

## EFFICIENT 1 × 16 OPTICAL POWER SPLITTER BASED ON InP

M. Zirngibl, C. Dragone, C. H. Joyner, M. Kuznetsov and U. Koren

*Indexing terms: Optical couplers, Integrated optics, Optical waveguide components*

An InP-based 1 × 16 optical power splitter is demonstrated. The device has 250 μm spaced output channels and a total length of 5·1 mm. This small size was realised by using a free-space radiative input-output coupling and specially designed 1·85 mm curvature S-bends. The worst case excess loss for TM and TE polarised light is 3 dB.

Transparent, linear networks based on optical wavelength-division multiplexing are believed to be the most practical solution for very large bandwidth communication [1]. This technique can take full advantage of the almost unlimited bandwidth of the optical fibre. One key device in such a network is an optical 1 × $N$ power splitter [2] which is used to combine the data stream from different transmitters and to distribute it to different receivers. $N \times N$ multiplexers and star couplers based on a radiative design have been successfully fabricated with $Si/SiO_2$ based glass waveguides [3]. The radiative approach is believed to be advantageous over Y-branch based design [4] because it allows the design of more compact devices. Also, Y-branches suffer from scattering losses due to the vertex [5]. We present a 1 × 16 radiative power splitter fabricated with InP-based waveguides. The high refractive index of compound semiconductors makes possible the use of tight bends which considerably reduces the overall size of the splitter as compared to $Si/SiO_2$ based devices. The possibility of integration with other optoelectronic components such as detectors, gain sections or lasers makes this approach attractive. As potential drawbacks of using InP, instead of $Si/SiO_2$-based waveguides, we note the increased polarisation sensitivity and also the more difficult fibre-waveguide coupling.

The arrangement considered here is illustrated in Fig. 1. The splitter design assumes a refractive index step $dn/n = 4{\cdot}2 \times 10^{-3}$. The 2·0 μm wide input waveguide radiates its power into the planar free-space region, which is a dielectric slab placed between the input waveguide and the receiving array of 16 waveguides. The efficiency of the device is given by the ratio of the power coupled into the waveguides and the total input power. The power radiated outside the receiving array aperture and the power lost due to the nonzero gaps between the waveguides thus reduce the efficiency from unity. For lithographical convenience, the minimum gap between adjacent waveguides was chosen to be 1·5 μm. To produce equal power distribution in all 16 waveguides, the receiving apertures are increased from 3 μm for the central waveguide to 10 μm for the outermost waveguide. This was done by calculating the field distribution at the receiving end of the 1 mm long free space region. The receiving waveguides ... the 16 output ports which are spaced by 250 μm ... to ... fibre coupling. In a first, straight section, the waveguide width is tapered down to the width of the S-bend. The bend radius of the outermost waveguides is 1·85 mm and increases gradually in each successive waveguide toward the central waveguides, so that the end points of all S-bends are aligned. The second and third outermost waveguides have 2·2 and 2·5 mm radii of curvature, respectively. To reduce the bend losses, the waveguide widths of the outer waveguides are increased up to 5·75 μm from the 3 μm widths of the central S-bends. Also, offsets at the straight-to-bend and bend-to-bend ... interfaces have been included [6] in the six outer waveguides. ... details on the bend design, refer to Reference ... The total length of the device is 5·1 mm.

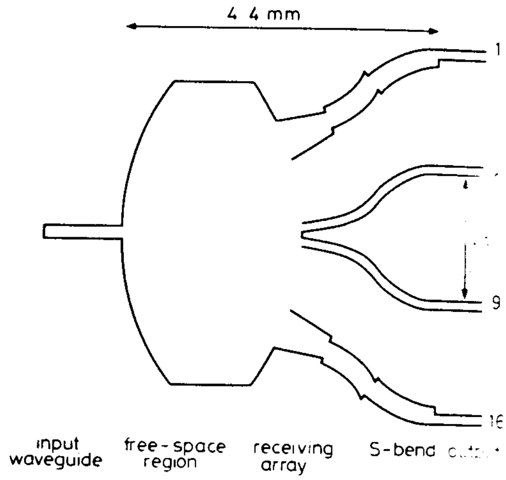


**Fig. 1** *Schematic design of 1 × 16 optical power sp...*

We used a buried-rib waveguide structure [8] as shown in Fig. 2. The lateral confinement is provided by a 400 Å lattice matched quaternary loading rib spaced by 150 Å InP on a 3000 Å quaternary guiding layer of the same composition. After a first growth, the rib is defined by a selective $H_2SO_4 : H_2O_2 : H_2O$ chemical etch and buried in InP by subsequent regrowth. Both growth steps are carried out by low pressure (100 torr) MOCVD. Conventional ... graphy and $SiO_2$ masking have been used for ... A bandgap wavelength of 1·35 μm has been measured by photoluminescence for the quaternary material. This gives an effective index step $dn/n = 4{\cdot}4 \times 10^{-3}$ which is slightly above the value taken for the design calculations. The straight waveguide losses are well below 1 dB/cm as determined by measuring the Fabry-Perot (FP) contrast ratios [9] in a straight test section. Indeed, samples up to 1 cm long showed FP contrasts of 3 which means that the loss over this distance is insignificant.

The power splitters were tested with 1·4... ...m a semiconductor laser diode. The light is coup... ... wave guide through a lensed fibre. A fibre polarisation controller allows us to select the input polarisation. The output light is collected by a ×40 microscope lens and coupled simultaneously into a multimode fibre for absolute power measure-

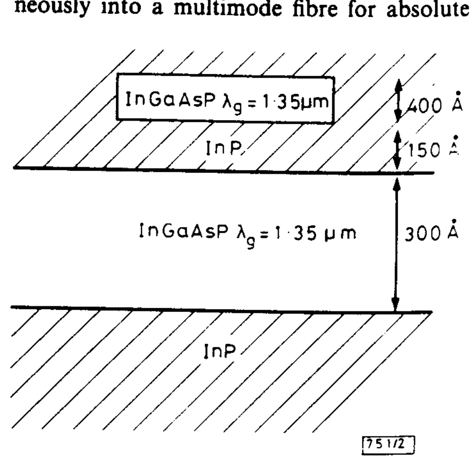


**Fig.** *Cross-section through waveguide structure*